



## Molecular Crystals and Liquid Crystals Science and Technology. Section A. Molecular Crystals and Liquid Crystals

Publication details, including instructions for authors and  
subscription information:

<http://www.tandfonline.com/loi/gmcl19>

### Photoexcitations in MX Chains: Dynamics of Solitons and Polarons in [Pt(en)<sub>2</sub>][Pt(en)<sub>2</sub>I<sub>2</sub>](ClO<sub>4</sub>)<sub>4</sub>

Hiroshi Okamoto <sup>a</sup>, Yasuo Oka <sup>a</sup>, Tadaoki Mitani <sup>b</sup>, Masahiro  
Yamashita <sup>c</sup> & Koshiro Toriumi <sup>d</sup>

<sup>a</sup> Research Institute for Scientific Measurements, Tohoku  
University, Katahira, Sendai, 980-77, Japan

<sup>b</sup> Japan Advanced Institute of Science and Technology, Ishikawa,  
923-12, Japan

<sup>c</sup> Graduate School of Human Informatics, Nagoya University,  
Nagoya, 464-01, Japan

<sup>d</sup> Department of Material Science and Technology, Hyogo,  
678-12, Japan

Version of record first published: 24 Sep 2006.

To cite this article: Hiroshi Okamoto , Yasuo Oka , Tadaoki Mitani , Masahiro Yamashita & Koshiro Toriumi (1996): Photoexcitations in MX Chains: Dynamics of Solitons and Polarons in [Pt(en)<sub>2</sub>][Pt(en)<sub>2</sub>I<sub>2</sub>](ClO<sub>4</sub>)<sub>4</sub>, Molecular Crystals and Liquid Crystals Science and Technology. Section A. Molecular Crystals and Liquid Crystals, 285:1, 303-310

To link to this article: <http://dx.doi.org/10.1080/10587259608030817>

PLEASE SCROLL DOWN FOR ARTICLE

Full terms and conditions of use: <http://www.tandfonline.com/page/terms-and-conditions>

This article may be used for research, teaching, and private study purposes. Any substantial or systematic reproduction, redistribution, reselling, loan, sub-licensing, systematic supply, or distribution in any form to anyone is expressly forbidden.

The publisher does not give any warranty express or implied or make any representation that the contents will be complete or accurate or up to date. The accuracy of any instructions, formulae, and drug doses should be independently

verified with primary sources. The publisher shall not be liable for any loss, actions, claims, proceedings, demand, or costs or damages whatsoever or howsoever caused arising directly or indirectly in connection with or arising out of the use of this material.

## PHOTOEXCITATIONS IN MX CHAINS:

### DYNAMICS OF SOLITONS AND POLARONS IN $[\text{Pt}(\text{en})_2][\text{Pt}(\text{en})_2\text{I}_2](\text{ClO}_4)_4$

HIROSHI OKAMOTO and YASUO OKA

Research Institute for Scientific Measurements, Tohoku University, Katahira, Sendai  
 980–77, Japan

TADAOKI MITANI

Japan Advanced Institute of Science and Technology, Ishikawa 923–12, Japan

MASAHIRO YAMASHITA

Graduate School of Human Informatics, Nagoya University, Nagoya 464–01, Japan

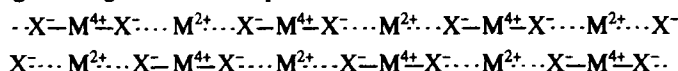
KOSHIRO TORIUMI

Department of Material Science and Technology, Hyogo 678–12, Japan

**Abstract** Dynamics of photo-induced gap states such as charged-solitons and polarons have been studied in the  $[\text{Pt}(\text{en})_2][\text{Pt}(\text{en})_2\text{I}_2](\text{ClO}_4)_4$  single crystal using the photo-induced ir absorption (PA) measurements. Annihilation processes of the gap states are well explained by the bimolecular recombination model. The PA intensities and the decay characteristics of both charged-solitons and polarons are strongly temperature-dependent. The temperature dependences of the rate constant of recombination for both carriers clearly show a crossover of the transport mechanism from hopping to tunneling with decrease of temperature.

## INTRODUCTION

The great tunability of the CDW states in the halogen( $X=\text{Cl}, \text{Br}, \text{I}$ )-bridged metal( $M=\text{Ni}, \text{Pd}, \text{Pt}$ ) complex (or equivalently the MX chain compound), has made this a model material for the study of photoexcitations under the influence of the strong electron–lattice (e–l) and electron–electron interactions in the one-dimensional (1-D) Peierls–Hubbard system.<sup>1,2</sup> Moreover, the broken symmetry degenerate ground states expressed as



lead to the prediction of spin-solitons and charged-solitons for the elementary excitations as well as polarons,<sup>3,4</sup> similarly to the conjugated polymers such as trans-polyacetylene  $((\text{CH})_x)$ .

Our previous measurements of photo-induced absorption (PA) on the MX chain compounds having different dimensionality of CDW ( $[\text{Pt}(\text{en})_2][\text{Pt}(\text{en})_2\text{X}_2](\text{ClO}_4)_4$  (en=ethylenediamine) and  $[\text{Pt}(\text{chxn})_2][\text{Pt}(\text{chxn})_2\text{X}_2]\text{X}_4$  (chxn=cyclohexanediamine)) have demonstrated that the two types of the gap states, namely, charged-solitons and polarons are photogenerated.<sup>5,6</sup> In

$[\text{Pt}(\text{en})_2][\text{Pt}(\text{en})_2\text{X}_2](\text{ClO}_4)_4$  ( $\text{X}=\text{Br}, \text{I}$ ) where the interchain interaction of CDW is weak, the midgap band named as **b** is observed at almost half of the gap energies, which is attributable to charged-solitons. In  $[\text{Pt}(\text{chxn})_2][\text{Pt}(\text{chxn})_2\text{X}_2]\text{X}_4$  ( $\text{X}=\text{Br}, \text{I}$ ) having two-dimensionally ordered CDW, photogeneration of solitons is suppressed. Besides the midgap band **b**, there have been observed two PA bands **a**<sub>1</sub> and **a**<sub>2</sub> insensitive to the dimensionality of CDW, which are assigned to polarons. Spectral shapes of these PA signals due to charged-solitons and polarons are found in agreement with those predicted by theoretical models.<sup>7,8</sup>

In this paper, we report the dynamics of the photo-induced gap states in  $[\text{Pt}(\text{en})_2][\text{Pt}(\text{en})_2\text{I}_2](\text{ClO}_4)_4$  on the basis of the excitation-power, time and temperature dependences of the PA signals. (Hereafter, this compound is expressed by Pt-I.) Our attention is focussed especially on the transport mechanism of the gap states. The excitation-power and time dependences of the PA signals could be explained by the simple bimolecular recombination model, and the intensity and the decay rate of the PA signals are found to be strongly dependent on temperature. From the analysis of the results in the framework of the bimolecular recombination model, we propose the two types of the transport mechanism, hopping and tunneling, for both charged-solitons and polarons, depending on temperature. These two types of mechanism are well interpreted by taking account of the e-l interactions and the quantum lattice fluctuations. Moreover, the origin of the photoconductivity will be discussed by comparing the activation energy of the photoconductivity with that of the recombination rate for photo-products, which can be derived from the temperature dependence of the PA signals.

## EXPERIMENTAL

The PA measurements were made by using a Fourier-transform infrared spectrometer (Nicolet system 800) equipped with an InSb detector. The experimental procedures to obtain PA spectra have been reported elsewhere.<sup>9</sup> As the excitation light, Ar laser (5145 Å) was used. The single crystal of the Pt-I compound was synthesized in the same way as reported in Ref.2 and mounted on the cold finger of an Air Products cryostat allowing control of the sample temperature between 300 K and 10 K.

## RESULTS AND DISCUSSIONS

The PA spectra  $\Delta\alpha$  (photo-induced change of  $\alpha(=kd)$ ) of the Pt-I single crystal for various temperatures were presented in Figure 1. Here, *k* and *d* are the absorption coefficient and the thickness of the sample, respectively. In the measurements, the power of the excitation lights was 5 mW/cm<sup>2</sup>, and both the excitation lights and the transmission lights are polarized parallel to the chain axis *b*. As previously reported in Ref.5, the structure **a**<sub>1</sub> and **a**<sub>2</sub> are assigned to polarons and the mid-gap structure **b** to charged solitons. With increase of temperature, intensities of the PA signals sharply decrease, and above 250 K, PA signals cannot be detected.

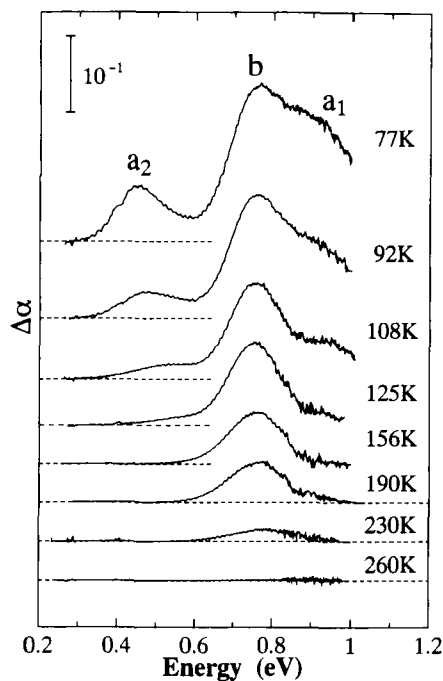


FIGURE 1 The photo-induced absorption spectra in the  $[\text{Pt}(\text{en})_2][\text{Pt}(\text{en})_2\text{I}_2](\text{ClO}_4)_4$  single crystal. Both of the transmission light and the excitation light (5145 Å) are polarized parallel to the chain axis b. The broken lines indicate  $\Delta\alpha=0$ .

Before a discussion about the temperature dependences of the PA signals, we will consider the annihilation process of the photo-products. As for this, the excitation-power dependence and the time characteristics of the PA signals give important informations. The integrated intensities of the PA signals  $I_{\text{PA}}$  have been evaluated as a function of the excitation power  $I_{\text{ex}}$  and the time  $t$  by fitting the sum of the three Gaussian bands to the obtained PA spectra. In Figure 2,  $I_{\text{PA}}$  is plotted against  $I_{\text{ex}}$  at 77K (open marks) and 130 K (solid marks). The data of  $I_{\text{PA}}$  are almost proportional to the square root of  $I_{\text{ex}}$  at both temperatures, as drawn by the dotted lines (77K) and the broken lines (130K), suggesting a bimolecular recombination of photocarriers. When neglecting the interaction between polarons and charged-solitons, the bimolecular recombination processes are simply expressed by phenomenological rate equations,

$$\frac{dN_p}{dt} = \Phi_p I - k_p N_p^2, \quad (1a)$$

$$\frac{dN_s}{dt} = \Phi_s I - k_s N_s^2, \quad (1b)$$

where  $N$  is the number of polarons or solitons per unit volume,  $I$  the photon number of excitation light per unit volume ( $I \propto I_{\text{ex}}$ ),  $\Phi$  the generation efficiency of photocarriers,  $k$  the rate constant of recombination. The  $p$  and  $s$  denote polarons and charged-solitons, respectively. The number of carriers in the steady state  $N_0$  ( $N_0^p$  for polarons and  $N_0^s$  for charged-solitons) is expressed as  $(\Phi_s I / k_{s,p})^{0.5}$ . The square root dependence of  $N_0^{s,p}$  on  $I$  agrees with the observed dependence of

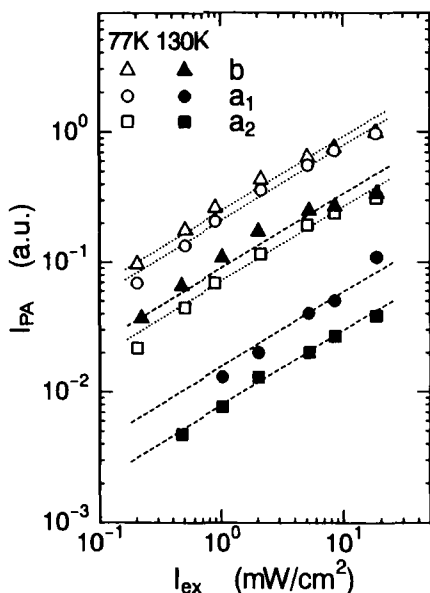


FIGURE 2 The integrated intensities  $I_{PA}$  of the PA bands  $a_1$  (circles),  $a_2$  (rectangulars), and  $b$  (triangles) as a function of the excitation power  $I_{ex}$  at 77K (open marks) and 130 K (solid marks). The dotted lines and the broken lines denote  $I_{PA} \propto I_{ex}^{0.5}$ .

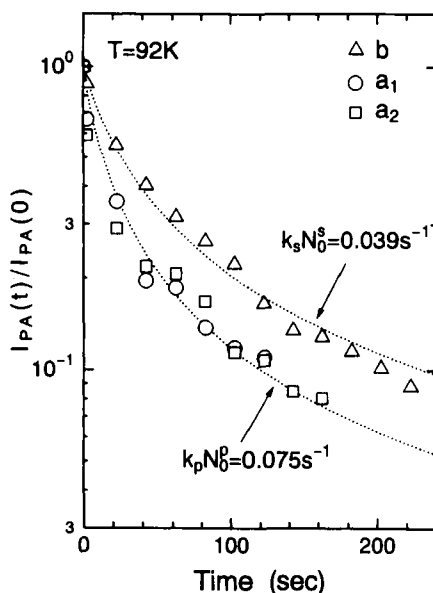


FIGURE 3 Time dependences of the normalized intensities of the PA signals at 92K. The dotted lines show the eq.(2) for the indicated values of  $k_s N_0^s$  and  $k_p N_0^p$ .

$I_{PA}$  on  $I_{ex}$ . The time dependences of  $N_{a,p}$  are expressed as following simple formula.

$$N_p(t)/N_0^p = (1 + k_p N_0^p t)^{-1} \quad (2a)$$

$$N_s(t)/N_0^s = (1 + k_s N_0^s t)^{-1} \quad (2b)$$

In Figure 3, time dependences of the integrated intensities of the PA signals  $I_{PA}$  at 92K are plotted in logarithmic scale. The charged-solitons detected as the  $b$  band are found to be longer lived than the polarons detected as the  $a_1$  and  $a_2$  bands. The time characteristics of the PA signals can be well reproduced by the broken lines using the eq.(2a,b) with the parameters  $k_s N_0^s$  for charged-solitons and  $k_p N_0^p$  for polarons given in Figure 3. This also demonstrates that the bimolecular recombination model is appropriate for both charged-solitons and polarons in the Pt-I compound.

So far, we have not considered the interaction between charged-solitons and polarons. A charged-soliton may coulombically interact with a oppositely charged-polaron. When they recombine, a spin-soliton will be produced. Such a recombination process, however, seems to be negligible in our case from the following reasons. As demonstrated in our previous studies,<sup>5</sup> the absorption band due to spin-solitons is observed as a single band with the energy of 0.82 eV, which is clearly discriminated from the PA band of charged-solitons around 0.75 eV and the two PA bands of polarons around 0.45 eV and 0.92 eV at 77 K. The spin-solitons are induced in as-grown samples probably due to the presence of the finite chains composed of the odd number of

Pt ions and therefore permanently exist, but their amount is extremely small (ca.  $10^{-4}$  per Pt site). If a spin-soliton was generated by the recombination of a charged-soliton and a polaron, the absorption for spin-solitons would be observed in the PA spectra. However, there are no PA signals due to spin-solitons in the PA spectra under nor after laser irradiations. Moreover, there is no evidence of the recombination between charged-solitons and polarons in the time characteristics of the PA signals. To take account of the recombination between a charged-soliton and a polaron, the term  $-k_r N_s N_p$  should be added in the rate equation (eq. (1a,b)). Here,  $k_r$  is the recombination rate between a charged-soliton and a polaron. In this case, the time characteristics of the PA signals necessarily deviate from the equation (2a,b). The experimental results are, however, clearly reproduced by the equation (2a,b) as shown in Figure 3. These facts suggest that the recombination rate  $k_r$  is much smaller than  $k_s$  and  $k_p$ . The reason why the recombination between a charged-soliton and a polaron hardly occurs, is not clear at the present stage. Further studies will be necessary to solve that.

Next problem is to clarify the transport mechanism of photocarriers. Important informations about that can be obtained from the temperature dependence of  $k_s$  and  $k_p$ . We measured the time dependences of the PA spectra at the various temperatures and evaluated the values of  $k_{s,p}$ . As mentioned above,  $N_0^{s,p} = (\Phi_{s,p} I / k_{s,p})^{0.5}$ , according to the bimolecular recombination model, so that temperature dependence of  $(N_0^{s,p})^{-2}$  or equivalently  $I_{PA}^{-2}$  reflects the temperature dependence of  $k_{s,p}$ , if the generation efficiency of photocarriers  $\Phi_{s,p}$  is independent of temperature. The linear relation between  $k_{s,p}$  and  $I_{PA}^{-2}$  can be examined by evaluating the  $k_{s,p}$  values at various temperatures. As shown in Figure 3,  $k_s N_0^s$  and  $k_p N_0^p$  are the fitting parameters to reproduce the time dependences of the PA intensities. Therefore, we displayed the relation between  $k_{s,p} N_0^{s,p} (\propto k_{s,p} I_{PA}^{-1})$  and  $I_{PA}^{-1}$  in Figure 4 for **b** and **a**<sub>2</sub> bands at the several temperatures. With increase of temperature, the values of both  $k_s N_0^s$  and  $k_p N_0^p$  increase showing that the decay of PA signals becomes fast. As clearly seen in Figure 4,  $I_{PA}^{-1}$  is proportional to  $k N_0$  for both carriers, that is,  $k$  is proportional to  $I_{PA}^{-2}$ . This linear relation demonstrates that the temperature dependences of generation efficiency of carriers,  $\Phi_s$  for charged solitons and  $\Phi_p$  for polarons, are negligible as compared with those of  $k_s$  and  $k_p$ , respectively. If  $\Phi_{s,p}$  was strongly temperature dependent, the temperature dependence of  $I_{PA}^{-1} (\propto (k_{s,p}(T)/\Phi_{s,p}(T))^{0.5})$  should not be equal to that of  $k_{s,p} N_{0s,p} (\propto (k_{s,p}(T)\Phi_{s,p}(T))^{0.5})$ .

We cannot obtain the values of  $k_p N_0^p$  (or  $k_p$ ) above 130 K and the values of  $k_s N_0^s$  (or  $k_s$ ) above 200 K, since the PA signals decay faster than the time resolution of our PA measurements (ca. 5 sec). It is, however, possible to evaluate the temperature dependence of  $k$  from those of  $I_{PA}$  in the higher temperature regions by assuming the linear relation between  $I_{PA}^{-2}$  and  $k$ .

Figure 5 is the Arrhenius plot of  $[I_{PA}(T)/I_{PA}(77K)]^{-2}$  for **a**<sub>1,2</sub> and **b** bands, which shows the temperature dependence of  $k_p$  for polarons and  $k_s$  for charged-solitons, respectively. In the temperature regions above 120 K for polarons and above 200 K for charged-solitons, the intensity of the PA signals remarkably decreases with increase of temperature. As seen in Fig.5,  $[I_{PA}(T)/I_{PA}(77K)]^{-2}$  in these high temperature regions almost follows the activation type formula  $[\exp(-\Delta/kT)]$  as plotted by the dotted lines. In the present case,  $k_{s,p} (\propto [I_{PA}/I_{PA}(77K)]^{-2})$  is

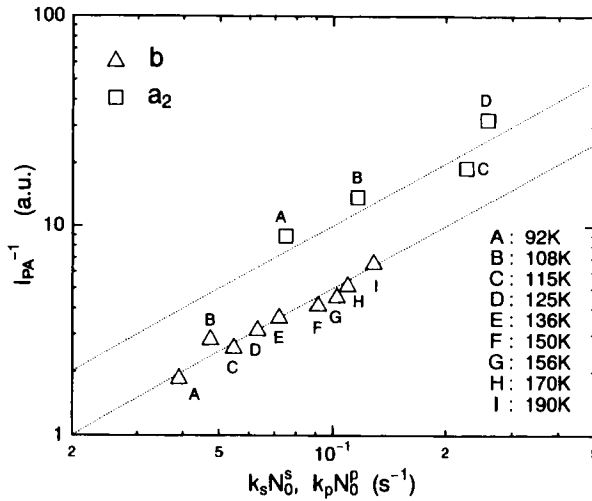


FIGURE 4 Relation between  $I_{PA}^{-1}$  and  $k_{s,p} N_0^{s,p}$ . The dotted lines indicate  $I_{PA}^{-1} \propto k_s N_0^s$  and  $k_p N_0^p$ .

determined by the encounter rate for photocarriers, so that the temperature dependence of  $k_{s,p}$  is considered to show the temperature dependence of the mobility of the photocarriers,  $\mu_s$  for charged-solitons and  $\mu_p$  for polarons. As a result,  $\Delta$  which is estimated to be  $0.76 \pm 0.1$  eV for charged-solitons and  $0.28 \pm 0.04$  eV for polarons as shown in Figure 5, corresponds to the activation energy of  $\mu_s$  and  $\mu_p$ , respectively. Namely, the carriers are bound to the lattice due to the e-l interaction. In the higher temperature region discussed here, a hopping mechanism dominates the transport properties of both charged-solitons and polarons.

The activation energy of the mobility for charged-solitons  $\mu_s$  is larger than that for polarons  $\mu_p$ . Such a difference can be qualitatively interpreted by taking account of the width of photo-products. When the width of a polaron or a charged-soliton increases, their pinning energy (the energy of the potential barrier for their transport) is expected to decrease. Considering that the width of a polaron is generally larger than that of a charged-soliton,<sup>10</sup> it is reasonable that the activation energy of  $\mu_p$  and  $\mu_s$ .

At the lower temperatures, i.e.  $T < 120$  K for polarons and  $T < 200$  K for charged-solitons, different mechanism should be considered for carrier transport, since the temperature dependence of  $[I_{PA}(T)/I_{PA}(77K)]^{-2}$  (or  $\mu_s$  and  $\mu_p$ ) is rather small. A reasonable interpretation for the transport mechanism in the low temperature regions is a tunneling process. The vibration relating to the transport process of polarons and charged-solitons is the stretching mode of the bridging iodine ions. According to the Raman measurements, the frequency of the symmetric stretching mode of the bridging iodine ions  $h\nu_s$  is ca.  $130 \text{ cm}^{-1}$ .<sup>11</sup> The temperature of the zero-point oscillation  $T_0 = h\nu_s/2$  is, therefore, 90K. As seen in Figure 5, the critical temperature  $T_c$  where the transport mechanism changes, is ca. 115 K for polarons, which is close to  $T_0$  (90K). It is quite natural that a crossover from a classical hopping process to a quantum tunneling process occurs with decrease of temperature. For charged-solitons, the critical temperature  $T_c \approx 200$  K is considerably larger



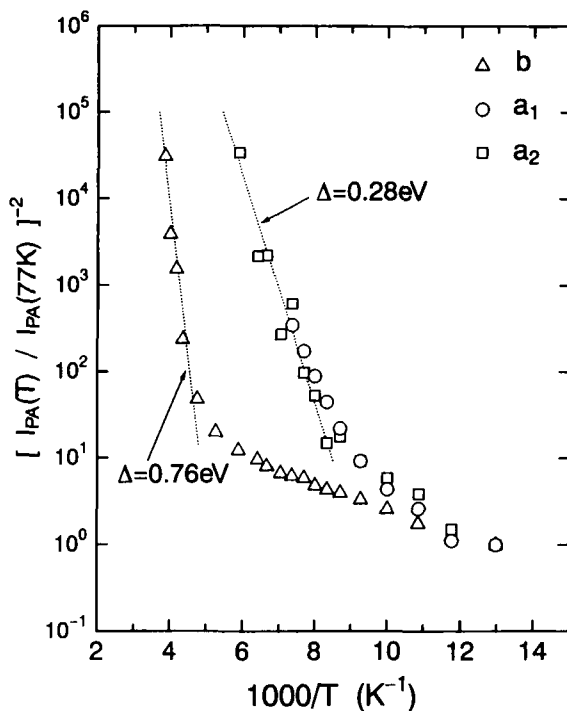


FIGURE 5 Temperature dependences of the normalized intensities of the PA signals  $[I_{PA}(T)/I_{PA}(77K)]^{-2}$ .

than  $T_0$ , so that a phonon-assisted tunneling process might be dominant for the transport.

Let's proceed to the discussion about the origin of the photoconductivities. The activation energy of photocurrent  $\Delta_{PC}$  along the chain axis  $b$  with the excitation light polarized parallel to  $b$  has been estimated about 0.32 eV in the temperature region from 300 K to 260 K.<sup>12</sup> In the measurements, the intensity of the excitation light  $I_{ex}$  was adjusted so that the photocurrent is proportional to  $I_{ex}$ . Below 260 K, the photocurrent could not be detected because of the limitation of the sensitivity. This value of  $\Delta_{PC}$  (0.32 eV) is almost equal to the activation energy of  $k_p$  or  $\mu_p$  (0.28 eV) for polarons obtained from the PA measurements. This indicates that polarons are responsible for the photoconductivities. In fact, it has been ascertained<sup>5</sup> that the excitation energy dependence of generation efficiency of polarons is the same as that of the photoconductivities.<sup>13</sup> Using the value of the mobility  $\mu_p$  along the chain axis  $b$  at 300 K ( $10 \text{ cm}^2\text{V}^{-1}\text{sec}^{-1}$ ) reported by Kurita et al.<sup>14</sup> and the obtained value of  $\Delta$  for polarons (0.3 eV), and extrapolating the data of  $[I_{PA}(T)/I_{PA}(77K)]^{-2}$  to 300 K, the mobility for polarons  $\mu_p$  at 92 K is estimated about  $5 \times 10^{-8} \text{ cm}^2\text{V}^{-1}\text{sec}^{-1}$ .

At last, we will note the difference of the dynamical properties of charged-solitons and polarons between  $\text{trans}-(\text{CH})_x$ <sup>15</sup> and the MX compound. In  $\text{trans}-(\text{CH})_x$ , the transfer energy  $T$  is much larger than the  $e$ - $I$  interaction energy  $S$ . In this case, charged-solitons and polarons moves freely along the chain and the interactions of the gap states with phonons determine their diffu-

sion constants.<sup>16,17</sup> In fact, the PA signals due to charged-solitons generated in a single chain decay in subpicosecond time scales by geminate recombinations, and those due to polarons decay within several tenth psec by encountering neutral solitons even at low temperatures.<sup>18</sup> On the other hand, in the MX compound, the e-I interaction  $S$  is comparable to  $T$ ,<sup>7,8</sup> so that solitons and polarons are localized with the finite pinning energies. In fact, when changing the bridging halogen ion from I to Cl, the effect of the e-I interaction increases and the decay of the PA signals has been found to become slower.<sup>19</sup> This is due to the increase of the potential barrier for transport of carriers induced by the increase of  $S/T$ .

In Summary, both of charged-solitons and polarons are long-lived in the Pt-I compound, suggesting their finite pinning energies. The temperature dependences of the rate constant for the bimolecular recombination,  $k_r$  for charged-solitons and  $k_p$  for polarons derived from the PA measurements, clearly show the crossover of the transport mechanism from the classical hopping process to the quantum tunneling process for both carriers. These behaviors of the gap states in the Pt-I compound are in contrast with those in  $\text{trans}-(\text{CH})_x$ . Finally, we emphasize again that the PA measurements presented in this paper directly detect the dynamical behaviors of charged-solitons and polarons, and enable us to study systematically the transport properties of photocarriers in the 1-D electron-lattice coupling systems.

The authors wish to thank Dr. Iwano and Prof. Nasu (KEK) for many enlightening discussions.

## REFERENCES

1. H. Okamoto, K. Toriumi, T. Mitani, and M. Yamashita, *Phys. Rev. B* **42**, 10381 (1990).
2. H. Okamoto, T. Mitani, K. Toriumi, and M. Yamashita, *Mater. Sci. Eng. B* **13**, L9 (1992).
3. Y. Onodera, *J. Phys. Soc. Jpn.* **56**, 250 (1987).
4. D. Baeriswyl and A.R. Bishop, *J. Phys. C: Solid State Phys.* **21**, 339 (1988).
5. H. Okamoto, T. Mitani, K. Toriumi, and M. Yamashita, *Phys. Rev. Lett.* **69**, 2248 (1992).
6. H. Okamoto and T. Mitani, *Prog. Theor. Phys.* **113**, 191 (1993).
7. J.T. Gammel, A. Saxena, I. Batistic, A.R. Bishop, and S.R. Phillpot, *Phys. Rev. B* **45**, 6408 (1992).
8. K. Iwano and K. Nasu, *J. Phys. Soc. Jpn.* **61**, 1380 (1992).
9. H. Okamoto, K. Okaniwa, T. Mitani, K. Toriumi, and M. Yamashita, *Solid State Commun.* **77**, 465 (1991).
10. A. Mishima and K. Nasu, *Phys. Rev. B* **39**, 5758 (1989); **39**, 5763 (1989).
11. R.J.H. Clark and M. Kurmoo, *J. Chem. Soc., Faraday Trans. 2* **79**, 519 (1983).
12. H. Okamoto et al., to be published.
13. M. Haruki, M. Tanaka, and S. Kurita, *Synth. Met.* **19**, 901 (1987).
14. S. Kurita, J. Ishikura, and M. Haruki, *Synth. Met.* **41**, 2785 (1991).
15. For a review, see A.J. Heeger, S. Kivelson, and J.R. Schrieffer, *Rev. Mod. Phys.* **60**, 781 (1988).
16. Y. Wada and J.R. Schrieffer, *Phys. Rev. B* **18**, 3897 (1978).
17. A. Terai and Y. Ono, *J. Phys. Soc. Jpn.* **55**, 213 (1986).
18. L. Rothberg, T.M. Jedju, S. Etemad, and G.L. Baker, *Phys. Rev. B* **36**, 7529 (1987).
19. H. Okamoto, Y. Oka, T. Mitani, K. Toriumi, and M. Yamashita, *Mol. Cryst. Liq. Cryst.* **256**, 161 (1994).